JTTEE 2:229-234

In-Flight Particle Surface Temperature Measurement: Influence of the Plasma Light Scattered by the Particles

P. Gougeon and C. Moreau

The application of optical pyrometry to low-melting-point plasma-sprayed particles can be limited by the plasma light scattered by the particles themselves. From spectroscopic measurements of the plasma between 650 and 1050 nm and using the Mie scattering theory, the intensity of scattered light has been determined in the case of nickel particles sprayed using an Ar/He plasma. The results show that, even in spectral regions between the atomic lines of the plasma gas, the scattered light can be important compared to the thermal emission of the particles. This scattered light leads to values of measured temperatures, which are all the more overestimated because the particle temperature is low and the particle/torch distance short. For a 50-μm nickel particle at 1550 °C, located 10 cm from the torch, the measurement error made with a double wavelength pyrometer is estimated at 100 °C.

1. Introduction

DUE to the complexity of interactions between particles and the plasma gas, on-line diagnostics are necessary to control the plasma spraying process.[1-3] One of the most useful diagnostics is the optical measurement of in-flight particle temperature, and such techniques have reached a high level of sophistication due to the development of high-speed electronics and low noise detectors. Measurement of the surface temperature in its present development is based on double wavelength pyrometry, rejecting the uncertainties related to the emissivity value and particle size. Monochromatic pyrometry used during the first steps of development of the technique was subject to these important uncertainties.[4]

However, there is another difficult point concerning the choice of spectral ranges used to measure the light emitted by the particles. This choice depends on three main factors: the spectral responsivity of the photodetectors, the sensitivity of the ratio of intensities emitted in the selected spectral ranges with the particle surface temperature; and the light intensity emitted by the hot particles compared to those coming from the plasma gas (direct or scattered) in the selected spectral ranges. This last factor has not been studied extensively,[5] and it is usually admitted that it is sufficient to fix the spectral ranges between the most intense atomic lines of the plasma gas. Although important, this condition is not sufficient because the plasma emission spectrum is not only composed of discrete atomic lines, but also of a continuous spectrum. Thus, the detected light is, in fact, the summation of the light emitted by the hot particles and the light emitted by the plasma.

This article is concerned with the evaluation of the light scattered by a particle irradiated by the plasma. This scattered intensity is determined from spectroscopic measurements of the plasma emission and the Mie scattering theory. The influence of the scattered light on the measurement accuracy of in-flight particle temperature is then investigated.

2. Theoretical Considerations

In-flight particle pyrometry involves the formation of an image of the emitting particles, when they pass across the measurement volume defined by the collection optics.[6,7] The collected radiation is composed of three components: the thermal radiation emitted by the particles under observation, the light emitted by the plasma contained in the measurement volume and directly collected by the detection optics, and the light scattered by the particles irradiated by the arc and the surrounding emitting gases.

Sakuta and Boulos[5] have studied the influence of the light emitted by the volume of hot gases observed by the collection optics. They defined a thermal visibility factor characterizing the ratio of particle emission over the emission of the volume of plasma. Based on theoretical considerations of plasma emission, they obtained different relations for the visibility of the particles as a function of the plasma and particle temperatures. However, this criterion does not take into account the quantity of plasma light scattered by the particles under observation and received by the detectors. Furthermore, from an experimental point of view, this scattered light is much more disturbing than the direct plasma light. Indeed, the signal resulting from the direct plasma light, being independent of the particle motion, has a different temporal evolution than the signals resulting from the two other light components (emitted and scattered). Although mentioned in the literature,[6,8] to the authors' knowledge, the influence of plasma light scattering on pyrometry accuracy has never been studied before.

Key Words: diagnostics, emissivity, light scattering, pyrometry, spectroscopy

P. Gougeon and **C. Moreau,** Industrial Materials Institute, National Research Council Canada, 75 boulevard de Mortagne, Boucherville, Quebec, Canada J4B 6Y4.

This work is based on a presentation made at the 1993 National Thermal Spray Conference, Anaheim, California, USA.

According to Planck's law, the emission of a particle (gray body assumption) is given by:

$$I_{em}(\lambda,T) = \varepsilon \frac{C_1}{\lambda^5} d^2 \frac{1}{\left[\exp\left(\frac{C_2}{\lambda T}\right) - 1\right]} d\lambda \quad [1]$$

where I_{em} is the emitted intensity, W/sr; λ is the wavelength, m; T is the surface temperature, K; ε is the emissivity; $C_1 = 9.352 \times 10^{-17}$ W · m^{-2}; $C_2 = 1.439 \times 10^{-2}$ m.K; and d is the diameter of the particle, m. The emitted intensity can be calculated from Eq 1 for different particle temperatures and diameters if the emissivity of the particle is known.

The particle under observation also scatters the plasma light in all spatial directions. The angular distribution of scattered intensity is not isotropic and depends on the particle size and light wavelength. In this work, the Mie theory is used to describe the light scattering by a spherical homogeneous particle, with a relative refractive index, $m = n - ik$, embedded in a nonabsorbing medium.[9]

From the Mie theory, the angular distribution of the scattered intensity I_{sca} (W/sr), far from the particle, is given by:

$$I_{sca} = \frac{\lambda^2}{\pi^3 d^2} P(\theta) P_{inc} \quad [2]$$

where θ is the scattering angle; $P(\theta)$ is the phase function given by the Mie theory; and P_{inc} is the light power incident on the geometric cross section of the particle. Equation 2 can be written:

$$I_{sca} = \gamma P_{inc} \quad [3]$$

where the Mie factor, γ, is calculated from the algorithm of Bohren[10] using the personal computer software developed by Corbin et al.[11]

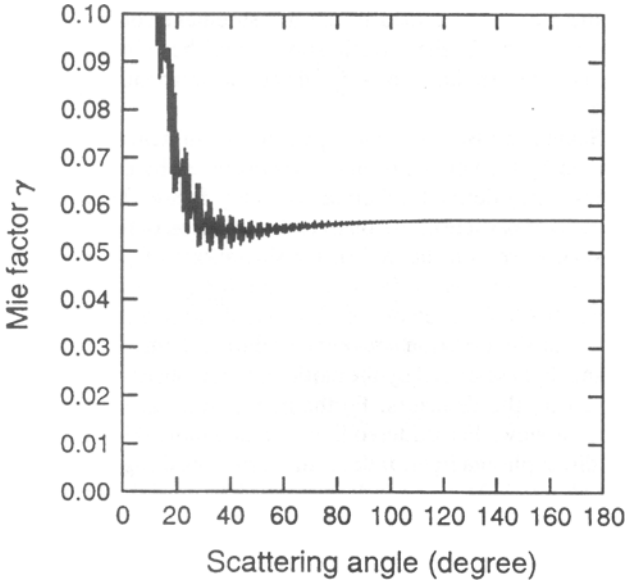

Fig. 1 Mie factor computed for a 50-μm nickel particle as a function of scattering angle.

The evaluation of the relative contributions of the scattered and emitted components of the collected light will be computed for nickel particles. Because the particle emissivity is not well known at high temperatures, a value of 0.5 is assumed. This value is realistic for metallic materials,[12] which can be oxidized in air plasma spraying. The value of complex refractive index, m, is taken equal to $2.81 - 4.99i$, which corresponds to the value for nickel at $\lambda = 995$ nm.[13] In these conditions and for particle diameters larger than 20 μm, there are no significant variations of γ for scattering angles larger than 60°. The dependence of γ with the scattering angle is shown in Fig. 1 for a 50-μm particle at $\lambda = 995$ nm. The evolution of the scattered intensity with the scattering angle is not smooth for small angles. The peaks in the curves are interpreted as due to the interference between the diffracted radiation and the radiation reflected from the surface of a homogeneous sphere. Practically, a small deviation to the particle sphericity, or a large collection angle, tends to smooth the shape of the curve (Fig. 1) even at small angles.[14] Typically, the angle of observation for plasma diagnostics is 90°, leading to a value of γ of 0.056. Using this value in Eq 3, the scattered light intensity can be determined from the measurement of the plasma light power incident on a particle. This incident power depends on the wavelength and the plasma conditions.

3. Experimental Setup

3.1 *Optical System*

The experimental setup for spectroscopic measurements is shown in Fig. 2. The light emitted by the whole plasma volume is collected by an optical fiber (diameter = 200 μm) at 34 cm from the front face of the plasma torch. The fiber numerical aperture (NA = 0.22) is large enough to collect all the light incident from the plasma. It is protected from sprayed particles and high-temperature gas by a glass window, and its axis makes an angle of about 7° above the torch axis (Fig. 2). This angle is com-

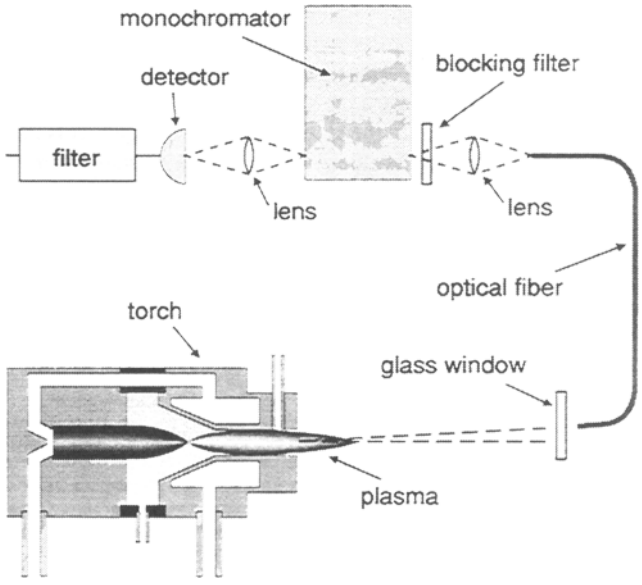

Fig. 2 Schematic of the experimental setup.

parable to the one made by the jet of sprayed particles relative to the torch axis. The intensity of the light received by the fiber is then comparable to the one incident on the particles at the same distance. The alignment of the fiber is made by looking for the maximum signal at 810 nm (intense argon line). The fiber output is focused on the entrance slit of a grating monochromator of focal length 1/8 m and throughput F/3.7 whose resolution is set to 4.3 nm. An optical long pass filter (blocking filter) at $\lambda = 610$ nm is interposed in front of the entrance slit to reject the grating second order. The grating rotation is driven by a continuous motor scanning the spectrum at a speed of 10.3 nm/s. The output slit of the monochromator is focused on the surface of a Si avalanche photodiode (APD) whose usable responsivity extends form 500 to 1100 nm.

3.2 *Acquisition System*

The detector signal filtered with a 100-Hz low pass filter is digitized using an A/D card installed in a microcomputer. The A/D conversion is done at a frequency of 1 kHz with 8-bit resolution. After each acquisition, the data are saved in an ASCII file for subsequent treatment with radiometric calibration data.

Table 1 Nickel spraying conditions

Arc gas flow rate	73.5 L/min
Arc current	750 A
Carrier gas flow rate	7.5 L/min
Powder feed rate	14 g/min
Particle size	+10 –44 μm

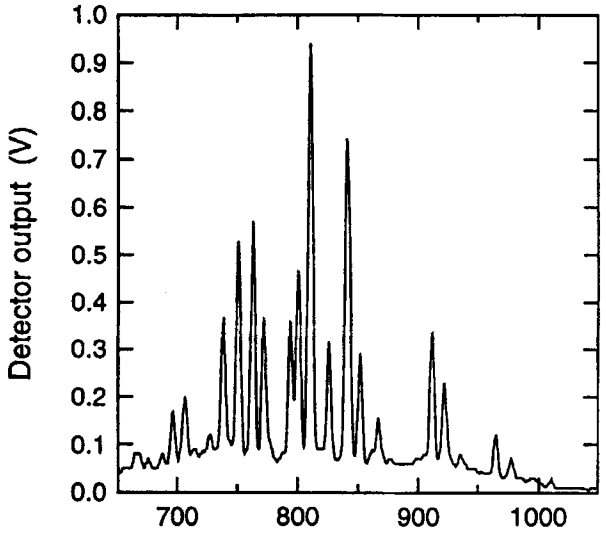

Fig. 3 Example of a recorded spectrum of an Ar/He plasma with nickel particles.

4. Results and Discussion

4.1 *Scattered Light Determination*

The spectroscopic measurements were carried out under the following conditions with nickel particles. The plasma gas was argon with helium as auxiliary gas (32 vol%), and the powder was fed with argon. The plasma torch, Plasmadyne SG-100*, was used in the configuration with the cathode 129, the anode 175, and the gas injector 113. Other spraying conditions are summarized in Table 1.

The optics transmission and detector responses limit the recording of the emission spectra to the 650 to 1050 nm range (Fig. 3). Except for a few nitrogen atomic lines, all of the lines present in this spectrum are atomic argon lines. In the spectral range under study, no nickel atomic lines were found in the plasma emission spectrum. However, nickel particles have a slight influence on the emission intensity because the signal recorded in the same plasma conditions, without particles, is 5 to 10% higher.

The absolute value of the power incident on the optical fiber is calculated by taking a radiometric calibration factor into account. This factor is obtained by comparing the signal received from a blackbody source (emissivity > 0.99) at 1500 °C with the corresponding spectrum given by Planck's law (Eq 1). The calibration factor takes into account the variation of the optical system response with wavelength, as shown in Fig. 4.

As described in Eq 3, the scattered intensity is proportional to the power incident on a particle. This power is computed from the spectrum shown in Fig. 3, using the calibration factor and taking into account the particle/source distance and the ratio of the particle to fiber cross sections. Because the optical measurements with the fiber cannot be carried out close to the plasma source, the intensity at closer distances (<34 cm) is assumed to

*Product of Miller Thermal, Inc., P.O. Box 1081, Appleton, WI 54912.

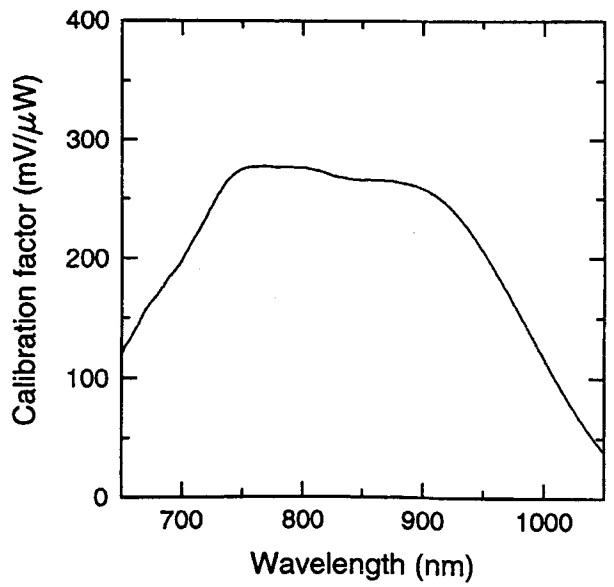

Fig. 4 Radiometric calibration factor of the optical system.

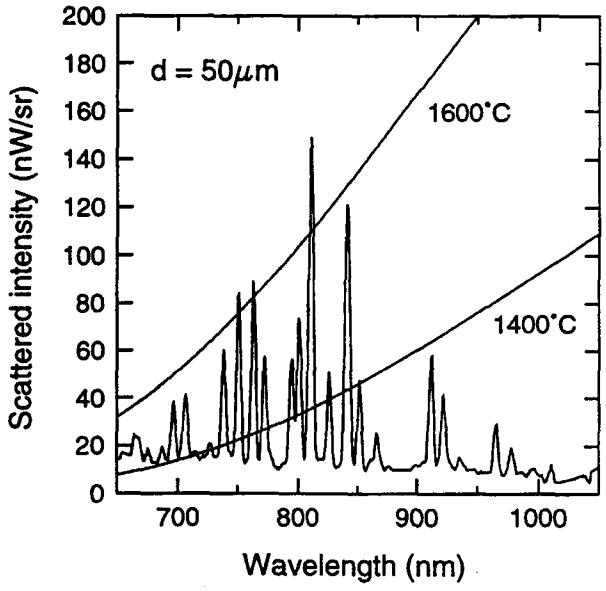

Fig. 5 Intensity scattered by a nickel particle at 10 cm from the torch. Comparison with the intensity emitted by the same particle at 1400 and 1600 °C.

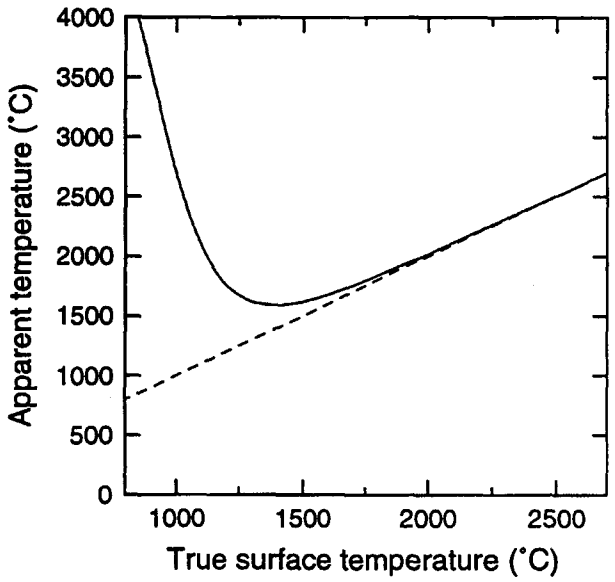

Fig. 6 Apparent temperature of nickel particles at 10 cm from the torch as a function of their true surface temperature.

vary with the square of the distance from the torch (point source assumption). The deviation from this law is all the more important because the particle is closer to the torch. However, considering the dimension of the plasma core, this law is assumed to correctly represent the variation of intensity for distances larger than 10 cm.

Figure 5 shows the light intensity scattered at 90° by a 50-μm particle at 10 cm from the torch as a function of wavelength. This scattered intensity is compared with the intensity emitted by the same particle at 1400 and 1600 °C in the same spectral interval ($d\lambda$ = 4.3 nm in Eq 1). It can be seen that plasma light scattering

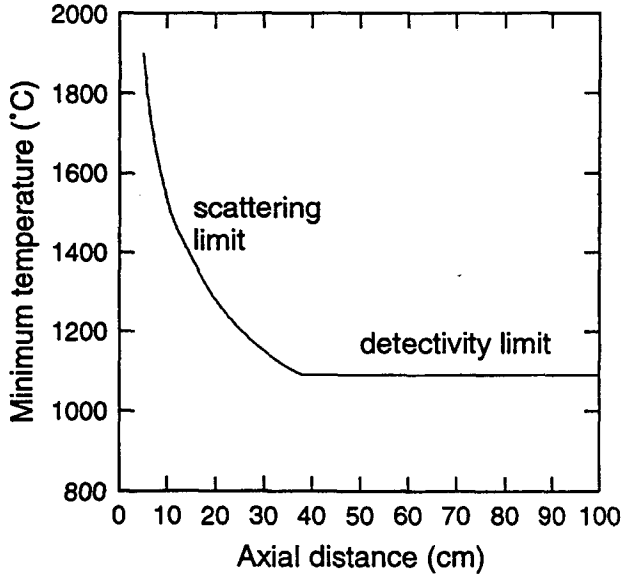

Fig. 7 Minimum measurable temperature for 50-μm nickel particles as a function of their distance to the torch.

is not negligible compared with particle emission at these temperatures, even in spectral ranges between the main atomic lines. The spectral ranges of a pyrometer must then be centered at long wavelengths to minimize the influence of the scattered light intensity. However, the temperature dependence of the detector responsivity, and its rapid decrease in the IR range, restrict the use of Si detectors at wavelengths shorter than 1020 nm.

4.2 *Scattering Limit*

Whatever the selected spectral ranges, the ratio of intensities in a two-wavelength pyrometer is affected by the presence of the scattered light, leading to an error in temperature measurement. This error is estimated from Fig. 5 by defining an apparent temperature, T_{app}. This temperature is defined by comparing the theoretical ratio of intensities emitted at λ_1 and λ_2 with the measured ratio, which takes into account the contributions of light scattered at each wavelength:

$$\frac{I_{em}(\lambda_1,T) + I_{sca}(\lambda_1)}{I_{em}(\lambda_2,T) + I_{sca}(\lambda_2)} = \frac{I_{em}(\lambda_1,T_{app})}{I_{em}(\lambda_2,T_{app})} \quad [4]$$

The variation of T_{app} with the temperature of a nickel particle located 10 cm from the torch is shown in Fig. 6. In this analysis of the pyrometric measurement error, the following spectral ranges are selected from Fig. 5: λ_1 = 995 nm ($\Delta\lambda_1$ = 50 nm), and λ_2 = 877 nm ($\Delta\lambda_2$ = 66 nm). The apparent temperature is then computed using Eq 4 and the spectrum of Fig. 5. The apparent temperature is higher than the true surface temperature and tends toward it at high temperature (dash line curve). Figure 6 shows that a particle at two different true surface temperatures may exhibit the same apparent temperature and therefore can be incorrectly analyzed. A minimum measurable temperature, T_{min}, can therefore be defined as being the true surface temperature, for which the measurement error is 100 °C. The minimum temperature is 1550 °C for a nickel particle of 50-μm diameter

at 10 cm from the torch (Fig. 6). This minimum depends on the scattered intensities and is also a function of the distance between the source (plasma torch) and the observed particles. When the particles are far from the torch, the contribution of the scattered light becomes negligible leading to a T_{min} decrease.

4.3 *Detection Limit*

There is another limit for the measurement of low temperature related to the detection of signals. Contrary to the light scattering limit, which does not depend on the nature of the pyrometric system, the detectivity limit changes with the detector and the transmission of optics. Although the characteristics of pyrometers can vary,[6,8,15] the constraints of measurement in plasma spraying conditions limit the possibilities. In this analysis, the detectivity limit is estimated for a typical double-wavelength pyrometer using interferential filters and Si avalanche detectors whose characteristics include: solid angle of collection (Ω) = 1.4×10^{-2} sr; transmission of optics (τ) = 30%; noise equivalent power (NEP) = 6.4×10^{-14} W/$\sqrt{\text{Hz}}$; and electrical bandwidth (Δf) = 10 MHz. The particle temperature is assumed to be measurable if the collected signal due to thermal emission is at least three times larger than the detector noise, i.e.:

$$\varepsilon \tau \Omega d^2 C_1 \frac{\lambda_1^{-5}}{\left(\exp\left(\frac{C_2}{\lambda_1 T}\right) - 1\right)} \Delta\lambda_1 \geq 3\text{NEP}\sqrt{\Delta f} \qquad [5]$$

from which one can obtain $T \geq 1090$ °C for 50-μm nickel particle. This minimum, being dependent on the NEP, is lower for systems using photomultiplier (PM) tubes as detectors. However, as PM responsivities are low at wavelengths longer than 850 nm, the spectral ranges should be chosen at shorter wavelengths where light scattering influence is more important (Fig. 5). Equations 4 and 5 can be used to determine whether the detection or scattering limit is reached first for the temperature measurement (Fig. 7). Near the torch, the plasma light scattering determines the limit for the temperature measurement, but above 38 cm from the torch, the limit depends on the pyrometer detection response.

5. Conclusion

From spectroscopic measurements of plasma light emission, it is possible to determine some limitations of the two-wavelength pyrometry applied to in-flight plasma-sprayed particles. Indeed, the plasma light scattered by the particles affects the accuracy of their temperature measurement. Even with a judicious choice of wavelengths, the scattered light limits the range of applicability of pyrometry toward low temperatures. The minimum measurable temperature is then a function of the particle/torch distance. At 10 cm from the torch, this minimum temperature is estimated at 1550 °C for 50-μm nickel particles sprayed with an Ar/He plasma. With Si avalanche detectors, the temperature measurement is limited by the detection characteristics of the optical system at distances larger than 38 cm. Even if their detectivity is lower than that of PM tubes, Si detectors must be preferred for measurement of low-temperature particles near the torch.

References

1. O.P. Solonenko, Complex Investigation of Thermophysical Processes in Plasma-Jet Spraying, *Pure Appl. Chem.*, Vol 62 (No. 9), 1990, p 1783-1800
2. J.R. Fincke, Diagnostics and Sensor Development for Thermal Spray Technologies, *Thermal Spray: International Advances in Coatings Technology*, C.C. Berndt, Ed., ASM International, 1992, p 1-9
3. P. Fauchais, J.F. Coudert, M. Vardelle, A. Vardelle, and A. Denoirjean, Diagnostics of Thermal Spraying Plasma Jets, *J. Thermal Spray Technol.*, Vol 1 (No. 2), 1992, p 117-128
4. B. Kruszewska and J. Lesinski, Temperature Distributions of Solid Particles in a Plasma Stream, *Rev. Phys. Appl.*, Vol 12, 1977, p 1209-1211
5. T. Sakuta and M.I. Boulos, Novel Approach for Particle Velocity and Size Measurement under Plasma Conditions, *Rev. Sci. Instrum.*, Vol 59 (No. 2), 1988, p 285-291
6. J. Mishin, M. Vardelle, J. Lesinski, and P. Fauchais, Two-Color Pyrometer for the Statistical Measurement of the Surface Temperature of Particles under Thermal Plasma Conditions, *J. Phys. E: Sci. Instrum.*, Vol 20, 1987, p 620-625
7. J.R. Fincke, C.L. Jeffery, and S.B. Englert, In-Flight Measurement of Particle Size and Temperature, *J. Phys. E: Sci. Instrum.*, Vol 21, 1988, p 367-370
8. S. Kuroda, T. Fukushima, S. Kitahara, H. Fujimori, Y. Tomita, and T. Horiuchi, Monitoring of Thermally Sprayed Particles using Thermal Radiation, The 12th International Conference on Thermal Spraying, The Welding Institute, Cambridge, UK, 1989, p 27/1-27/9
9. M. Kerker, *The Scattering of Light and Other Electromagnetic Radiation*, Academic Press, 1969
10. C.F. Bohren and D.R. Hufman, *Absorption and Scattering of Light by Small Particles*, John Wiley & Sons, 1983
11. F. Corbin, G. Grehan, G. Gouesbet, and B. Maheu, Interaction between a Sphere and a Gaussian Beam: Computations on a Micro-Computer, *Particle Particle Systems Characterization*, Vol 5 (No. 3), 1988, p 103-108
12. Y.S. Touloukian and D.P. DeWitt, *Thermal Properties of Matter*, Vol 7, IFI/Plenum, 1970, p 413-472
13. E.D. Palik, *Handbook of Optical Constants of Solids*, Academic Press, 1985, p 313-323
14. A. Ungut, G. Grehan, and G. Gouesbet, Comparisons between Geometrical Optics and Lorenz-Mie Theory, *Appl. Opt.*, Vol 20 (No. 17), 1981, p 2911-2918
15. C. Moreau, P. Cielo, M. Lamontagne, S. Dallaire, and M. Vardelle, Impacting Particle Temperature Monitoring during Plasma Spray Deposition, *Measure. Sci. Technol.*, Vol 1, 1990, p 807-814